A Comprehensive Review of the Slope Parameter Based Approach to Cathodic Protection Design and Analysis

W.H. Hartt and D.K. Lysogorski
Center for Marine Materials
Department of Ocean Engineering
Florida Atlantic University – Sea Tech Campus
101 North Beach Road
Dania Beach, Florida 33004 USA

Abstract

Advent and development of the Slope Parameter (total circuit resistance – cathode surface area product) during the past decade is proving to be an important milestone in cathodic protection design and analysis. This paper reviews the Slope Parameter concept and its underlying principles and provides examples in different categories to which it can be applied. Demonstrated also is utility of the methodology upon which the parameter is based to both galvanic and impressed current cathodic protection systems. Example categories include the following: 1) structures in low resistivity electrolytes with distributed anodes (offshore petroleum production platforms), 2) structures with high resistivity electrolyte exposure (reinforcing steel in atmospherically exposed, chloride contaminated concrete), and 3) submerged or buried one dimensional systems (pipelines and risers).

Key words: Cathodic protection, Slope Parameter, design, offshore structures, reinforced concrete, pipelines

General

While the inception and early development of cathodic protection (cp) was based upon remarkably insightful scientific studies [1-3], its subsequent evolvement and application has been incremental and based largely upon trial and error. Nonetheless, cathodic protection has become the primary corrosion control methodology for buried and submerged components and structures and for reinforcing steel in atmospherically exposed Cl^- contaminated concrete (for example, see references 4-6). Of particular recent significance is development of the Slope Parameter approach to cathodic protection design and analysis [7-10]. The basis for this, as was the case in earlier developed approaches [4,5], is Ohm's law,

$$I_a = \frac{f_c - f_a}{R_t}, \qquad (1$$

where I_a is anode current output, f_c and f_a are the closed circuit structure and anode potentials, respectively, and R_t is total circuit resistance. Figure 1 illustrates these parameters and the associated polarization curves for both anode and structure schematically. Upon solving for f_c [11] and expressing in terms of structure current density, i_c,

$$f_c = (R_t \cdot A_c) \cdot i_c + f_a, \qquad (2$$

where A_c is structure surface area. This projects a linear interdependence between f_c and i_c with slope $R_t \cdot A_c$ and vertical intercept f_a provided R_t, A_c, and f_a are constant for the time span to which the f_c and i_c data pertain. The $R_t \cdot A_c$ term is commonly referred to as the Slope Parameter, S. Also assumed is that f_c is spatially invariant.

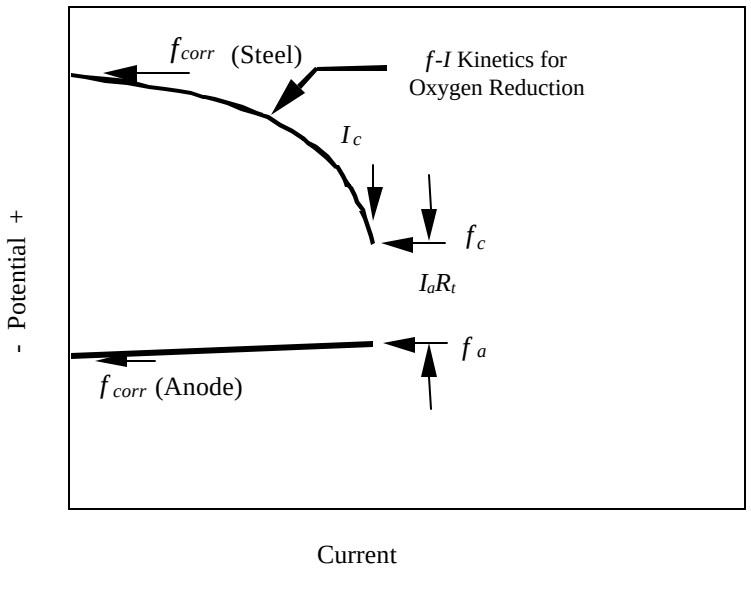

Figure 1: Schematic illustration of a polarization diagram and of parameters relevant to galvanic anode cathodic protection system design.

Applications of Equation 2

The above conditions for applicability of Equation 2 are normally realized for three dimensional structures with distributed anodes in low resistivity electrolytes such as offshore petroleum production platforms. In this regard, Kennelley and Mateer [12] reported polarization data for a production jacket structure in 162 m Gulf of Mexico water. The cp design was based upon 265 330 kg Al-Zn-In anodes with ones at the -37m and -105 m depths being instrumented for data acquisition; and f_c and i_c were recorded for the initial 7,000 hours of deployment. Figure 2 presents f_c-i_c data along with results for a 41 cm^2 API-Grade 42 steel specimen (A_c = 41 cm^2) polarized by a single Al-Zn-Hg anode in quiescent natural sea water under laboratory conditions, where a 450 Ohm resistor was in series between the anode and cathode [13]. Both sets of data transcend with time from upper right to lower left, such that initial structure potential and current density were approximately –0.66 V_{SCE} and 235 mA/m^2, respectively, and after 7,000 hours –0.98 V_{SCE} and 50 mA/m^2. Two methods are available for determination S, where the first utilizes the equation,

$$S = \frac{f_{c(i)} - f_a}{i_{c(i)}}, \qquad (3$$

where $i_{c(i)}$ is the initial current density and $f_{c(i)}$ is the corresponding structure potential; and the second is based upon the expression,

$$S = \frac{R_a \cdot A_c}{N}, \qquad (4$$

where R_a is resistance of an individual anode and N is the number of anodes. For the Kennelley and Mateer data, Equation 3 yields 1.79 $\Omega \cdot m^2$ and Equation 4 1.79 $\Omega \cdot m^2$. The graphically measured slope for the laboratory specimen data, on the other hand, gives S = 1.75 $\Omega \cdot m^2$. The Slope Parameter in this case was also calculated from the expression,

$$S \sim R_x \cdot A_c, \qquad (5$$

from which a value of 1.83 $\Omega \cdot m^2$ was determined. Thus, the two sets of determinations for each of the two

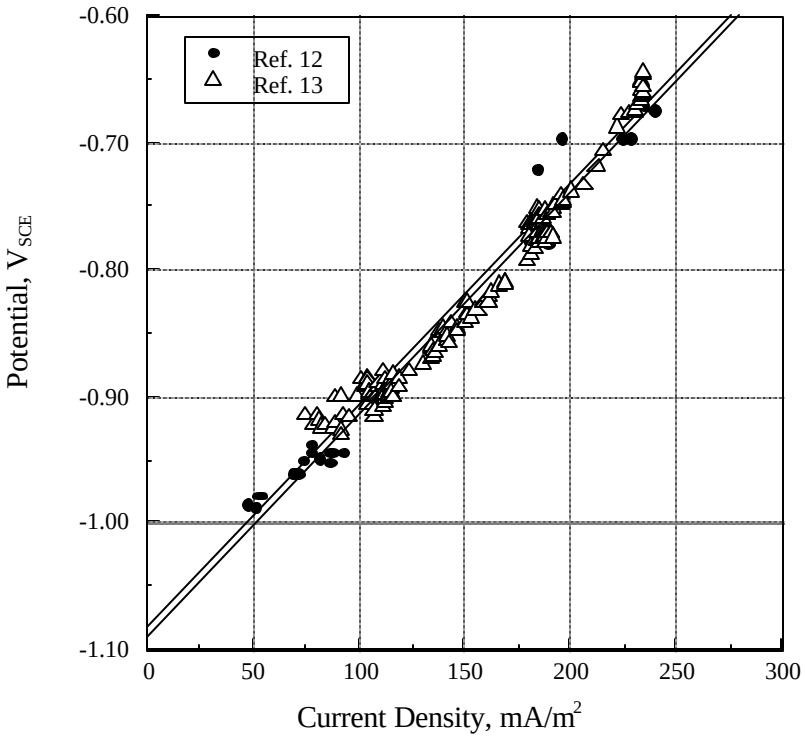

Figure 2: Potential versus current density for a laboratory specimen and an offshore structure.

cathodes are in excellent mutual agreement; and so cathodes of vastly difference surface area can be compared directly.

Reinforcing steel in concrete that is cathodically polarized by galvanic arc sprayed Zn exemplifies a system less applicable to satisfying any linearity constraint placed upon Equation 2. This arises because, first, R_t and f_a are likely to vary with time, the former by orders of magnitude in conjunction with concrete aging and relative humidity variations and the latter from possible anode passivation, and, second, reduced emphasis is placed on f_c since protection criteria are generally based upon the magnitude of polarization or depolarization rather than potential per se [14]. Consequently, the utility of Equation 2 for such situations necessarily focuses upon analysis of data acquired either at a particular time or over a time period during which R_t and f_a are relatively constant.

The above limitations aside, sufficient data for concrete structures are seldom reported to permit evaluation in terms of Equation 2. An exception is a study reported by Sagüés and Powers [15] of the cp system for the substructure for the Bahia Honda Bridge which crosses virtually open sea water in the Florida Keys [16]. The sprayed Zn system employed here included embedded steel probes (surface area 0.0013 m^2) for depolarization testing and i_c determinations at the 0.76, 1.22, 1.83, and 2.44 m elevations above mean high tide. Table 1 lists data for the 0.76 m elevation at three different times subsequent to energizing and Table 2 for four elevations 6.9 months after energizing. Of interest here is the relatively good correspondence between the measured and

Table 1: Listing of galvanic anode cp data at the 0.76 m elevation at different exposure times for the Bahia Honda Bridge.

Time,	Resist.,	f_c,	f_a,	i_c,	S ($R_t \cdot A_c$), $\Omega.m^2$	
months	Ω	mV_{CSE}	V_{CSE}	mA/m^2	Calculated	Measured
1.4	460	-630	-0.722	156	0.59	0.60
6.9	460	-759	-0.889	222	0.59	0.60
12.4	2,700	-463	-0.477	3.55	3.94	3.51

Table 2: Data for different elevations of the Bahia Honda Bridge 6.9 months subsequent to energizing the cp system.

Elevation, m	Resistance, Ω	f_c, V_{CSE}	f_a, V_{CSE}	i_c, mA/m^2	S ($R_t \cdot A_c$), $\Omega.m^2$	
					Calculated	Measured
0.76	460	-759	-889	222	0.59	0.60
1.22	1,200	-503	-551	31	1.54	1.56
1.83	1,400	-432	-459	15	1.80	1.82
2.44	1,200	-296	-336	25	1.60	1.56

calculated values for S, as shown in the last two columns of both tables. The former (measured value) was determined directly from the reported anode-to-probe resistance and the probe surface area and the latter (calculated value) using Equation 2.

The Unified Design Equation

Combining Equation 4 with the modified Faraday's law expression for design of galvanic cp systems [4,5],

$$N = \frac{i_m \cdot A_c \cdot T}{u \cdot C \cdot w}, \qquad (6$$

where,

i_m is the mean current density,
T is design life,
u is an anode utilization factor,
C is anode current capacity, and
w is weight of an individual anode,

yields what has been termed the Unified design Equation [8-10],

$$R_a \cdot w = i_m \cdot T \cdot K \cdot S, \qquad (7$$

where K is anode consumption rate (inverse of C). Of the parameters on the right side of Equation 7, i_m and S are determined by the nature of the exposure and K is a material property. As such, these, along with T can be considered as design choices. Consequently, the value for the right side is defined; and the cp design process reduces to designing or selecting an optimized anode such that the product of R_a and w equals the right side with R_a and w being optimized. The number of anodes is then determined from Equation 4.

Equation 7 has particular utility for cp design of marine structures because of the associated current density reduction with time that results from formation of calcareous deposits [13,17-23]. Consequently, a sigmoidal steady-state dependence of f_c upon i_c results when data for multiple specimens and a range of initial current densities (S values) are plotted. Figure 3 illustrates an example of this behavior. Such a trend defines the principle, if not the mechanism, for "rapid polarization" [24-29] in that the current density which ultimately results from modest cathodic polarization, (steady-state f_c of about-0.80 $V_{Ag/AgCl}$) is achieved only in the long-term, is approximately 2.5 times greater than if the long-term potential were near -1.00 $V_{Ag/AgCl}$. Correspondingly, Figure 4 illustrates incorporation of this phenomenon into the design process in terms of four cp design alternatives (choices for S) in relation to the dynamic and steady-state polarization curves. Thus, design according to S_1 results in under-protection and S_2 in protection but at a relatively high i_c. Designs in the range S_3-S_4, on the other hand, are optimum in that protection is adequate and i_c minimum.

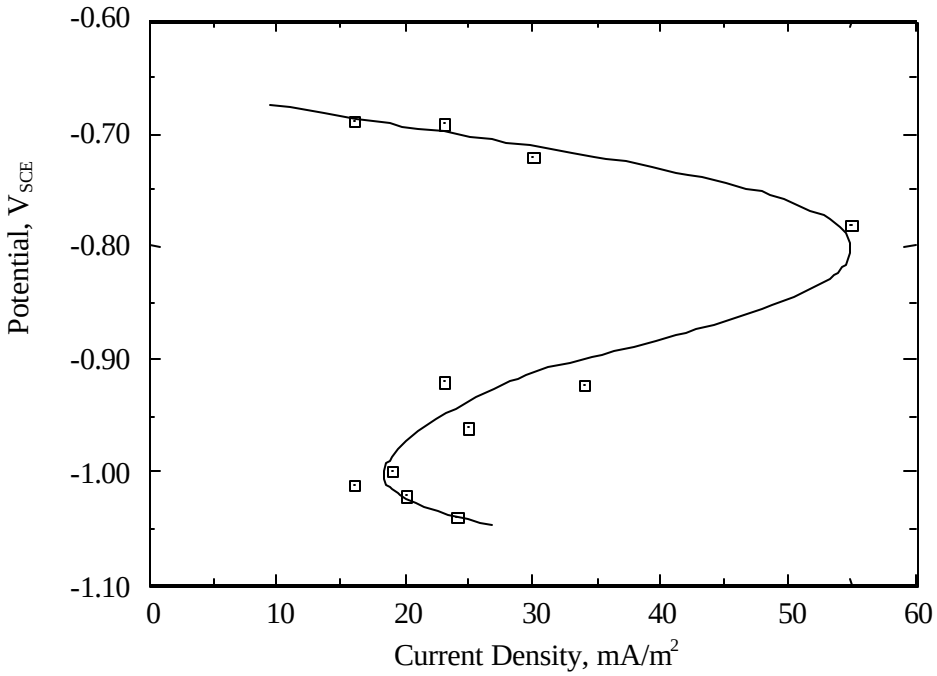

Figure 3: Long-term f_c-i_c relationship for steel in sea water as determined from laboratory experiments in ambient natural sea water [13].

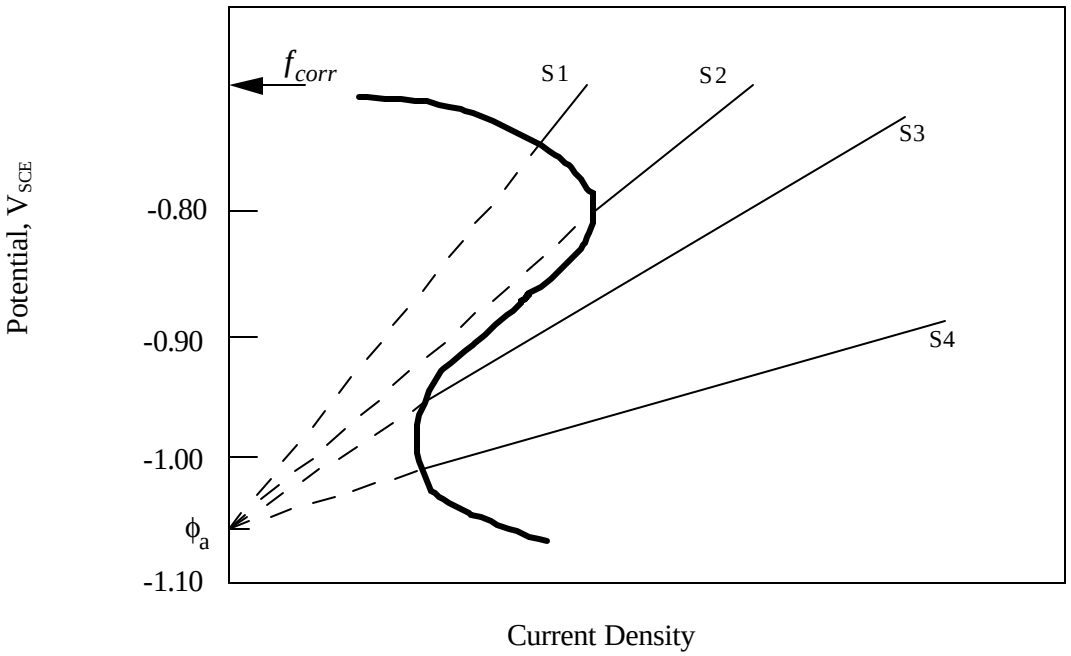

Figure 4: Schematic illustration of alternative design slopes in perspective to the long-term f-$_c i$ curve.

Impressed Current CP Systems

Equations 2-7 relate to galvanic anode cp systems; however, the impressed current case can be addressed using the relationship,

$$f_c = S \cdot i_c + f_a(eq), \qquad (8$$

where $f_a(eq)$ is the potential that would have to be realized by a galvanic anode if it were to provide the same current as an impressed current one ($f_a(ic)$) [30]. For this, it has been shown that,

$$V = f_a(ic) + (-f_c) + V_m, \quad (9$$

where V is rectifier voltage and V_m sums any other voltage drops in the circuit (lead wires and contacts, for example).

One-Dimensional Systems (Pipelines and Risers)

The polarized potential distribution for one dimensional structures is more complex that for space frame ones because anodes are normally discrete as opposed to distributed. Figure 5 schematically illustrates the potential that normally occurs for a marine pipeline that is polarized by galvanic bracelet anodes, and Figure 6 does the same for a buried onshore pipeline polarized by an impressed current system. In the former case, weight limitations for individual anodes are imposed by structural considerations and by deployment methods such that spacing between anodes is relatively short. Consequently, f_c is constant except within the anode potential field which typically extends about 10-15 m. For the situation in Figure 6, however, anode mass is not a factor; and anode bed spacing, as limited by the metallic return path voltage drop, is normally the controlling design parameter. Consequently, f_c becomes progressively more positive with increasing distance from the anode bed.

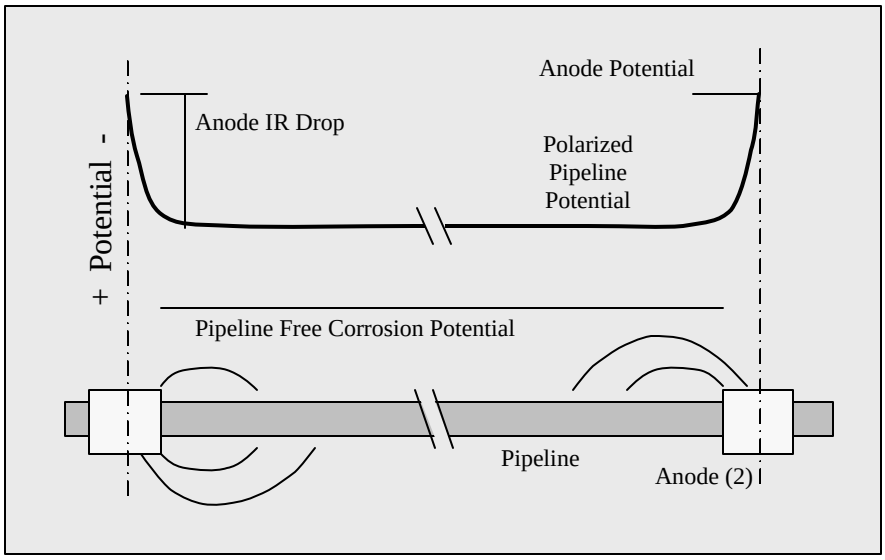

Figure 5: Schematic illustration of the potential profile that arises from galvanic cp of marine pipelines with bracelet anodes.

The present, common approach to marine pipeline initial cp design [4,31] is based upon 1) calculation of the number of bracelet anodes, N, according to,

$$N = \frac{I_c}{I_a}, \quad (10$$

2) application of Equation 1, 3) determination of pipe current demand, I_c as,

$$I_c = A_c \cdot f_c \cdot i_c, \quad (11$$

where f_c is the coating breakdown factor (ratio of bare to total surface area), and 4) determination of the requisite anode mass from Equation 6. Recently, however, a modified approach has been proposed based upon Equation 2

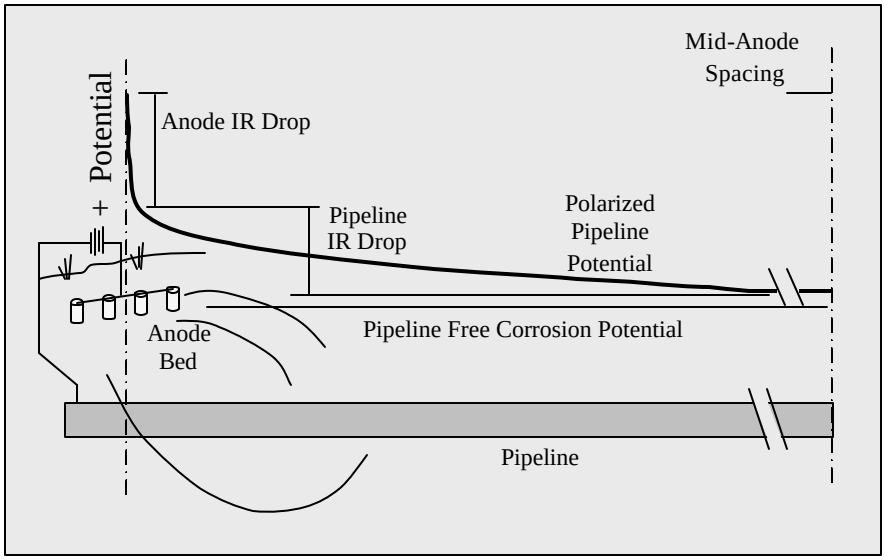

Figure 6: Schematic illustration of the potential profile that typically arises for buried pipelines polarized by an impressed current system anode ground bed.

and the assumptions that 1) anode spacing, L_{as}, is sufficiently small that metallic path resistance is negligible, 2) pipe resistance to sea water is negligible, 3) all current enters the pipe at coating holidays, 4) the f_c-i_c relationship is linear with slope a, and 5) f_c and f_a are constant with both time and position [32]. The resultant expressions,

$$f_c = \frac{f_{corr} + (f_a \cdot Y)}{1+Y}, \qquad (12$$

where f_{corr} is the pipe corrosion potential and

$$y = \frac{a \cdot g}{2p \cdot r_p \cdot L_{as} \cdot R_a}, \qquad (13$$

where g is the inverse of the coating breakdown factor and r_p is the pipe radius. Also, design life, T, was expressed as,

$$T = \frac{w \cdot C \cdot u \cdot a \chi g}{(f_{corr} - f_c) \cdot 2p \cdot r_p \cdot L_{as}}. \qquad (14$$

Table 3 lists a range of f and i_m values and shows the corresponding $a \cdot g$. Since the term $2p \cdot r_p \cdot L_{as} \cdot R_a / g$ (Equation 13) is, as the product of resistance and area, equivalent to S, this approach is termed the Slope Parameter method for pipeline cp design. Other Equation 12/13 parameters upon which the approach is based are 1) magnitude of polarization (f_{corr}–f_c), 2) driving potential (f_c-f_a), and pipe current demand (a).

This approach was demonstrated for a pipeline with the design choices listed in Table 4 and assuming 1) a standard 60.8 kg bracelet anode of length 0.432 m and outer radius 0.187 m, 2) f_c = -0.975 $V_{Ag/AgCl}$ (this constitutes a design polarized potential), and 3) R_a = 0.353 Ω, as determined from McCoy's formula [33] assuming 0.80 Ω·m electrolyte resistivity, as might typify a sea mud exposure. On this basis, L_{as} was calculated as 115 m (Equation 12) and T as 44 years (Equation 14). An improved match between the design and calculated T could be realized by iteration between Equations 12/13 and 14 using alternative choices for w (or R_a), a, g, or L_{as} (or for a combination of two or more of these terms).

Table 3: Listing of a range of ag values as related to coating quality and pipe bare area current density demand.

Pipe Bare Area, percent	f_c	g	i_m, mA/m^2	a, Ωm^2*	ag, Ωm^2
0	0	8	5	70	8
			20	10	
			50	7	
0.01	0.0001	10,000	5	70	700,000
			20	10	100,000
			50	7	70,000
0.1	0.001	1,000	5	70	70,000
			20	10	10,000
			50	7	7,000
1	0.01	100	5	70	7,000
			20	10	1,000
			50	7	700
5	0.05	20	5	70	1,400
			20	10	200
			50	7	140
100	1	1	5	70	70
			20	10	10
			50	7	7

* Alpha was calculated based upon the indicated i_c corresponding to 0.35 V polarization.

Figure 7 shows the projected f_c for both the original and final anode sizes (length and radius in the latter case were 0.209 and 0.160 m, respectively). Here, f_c based upon the initial design was –0.975 $V_{Ag/AgCl}$ by choice (L_{as} was calculated using this value) and upon the final –0.943 $V_{Ag/AgCl}$, the latter being determined by Equation 12 for f_c based upon L_{as} = 115 m and the final anode dimensions). Also illustrated are the attenuation profiles from a Finite Difference Method (FDM) solution to an inclusive, first-principles based attenuation equation that, first, was derived for the case of pipelines with identical, equally spaced superimposed anodes and, second, includes all relevant resistance terms (anode, coating (g), polarization (a), and metallic path) [34,35].

Projections from the Slope Parameter method (Equations 12/13) are seen to be in good agreement with the FDM solutions except in the immediate vicinity of the anode. The metallic path resistance can be considered negligible as indicated by the fact that the FDM solution projects constant f_c beyond the anode potential field.

Recently, a modified form of Equation 13 that includes metallic path pipe return resistance was derived as,

Table 4: Listing of pipe and electrolyte properties and design choices used in the example.

Pipeline Outer Radius, m	0.136
Pipeline Inner Radius, m	0.128
Electrolyte Resistivity, Ohm-m	0.80
Alpha, Ohm-m^2	7.5
Gamma	20
Design Life, years	30
Anode Current Capacity, Ah/kg	1,700
Anode Utilization Factor	0.8
Open Circuit Anode Potential, $V_{Ag/AgCl}$	-1.05

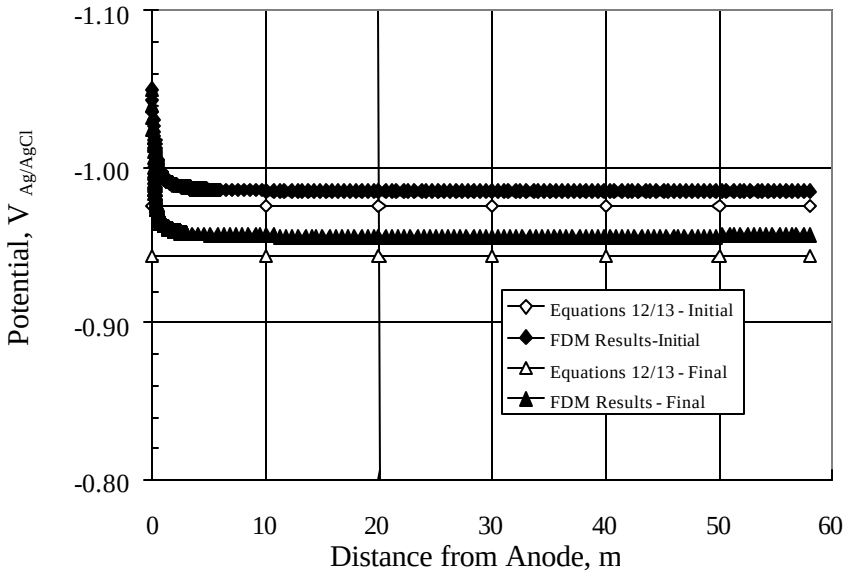

Figure 7: Potential profile projected by Equation 12/13 and by an FDM solution to an inclusive attenuation equation based upon initial and assumed final anode sizes.

$$Y = \frac{a \times g}{2 \cdot p \cdot r_p \cdot L_{as} \cdot \left(R_a + \frac{L_{as} \cdot R_m}{8} \right)}, \qquad (15$$

where R_m is pipe resistance per unit length [36]. This expression retains, however, the assumption that f_c is constant.

Potential attenuation projections based upon Equation 12/13, with and without inclusion of the metallic path resistance term (Equation 13 and 15, respectively) have also been compared to those from the inclusive equation, as shown in Figure 8 for the pipe and environment parameters listed in Table 5 and anode spacings of 500, 1,000, and 5,000 m. Here, electrolyte resistivities, r_e, typical of both sea water (0.30 Ω·m) and sea mud (1.0 Ω·m) are represented. In the lower resistivity case (Figure 8a), the inclusive equation indicates that metallic path voltage drop is significant only for the 5,000 m L_{as} case, where approximately one-half of the attenuation is associated with the anode and the other half with the metallic pipe. In the higher resistivity electrolyte example (Figure 8b), about 75 percent of the attenuation occurs in conjunction with the anode. For both r_e values, the far field potential projected by the solutions to the inclusive equation and Equation 12/15 are essentially the same, whereas that for Equation 12/13 is non-conservative.

A more general inclusive equation has recently been proposed that incorporates instances where identical, equally spaced anodes are offset from the pipeline, as is likely to occur for onshore buried applications and offshore retrofits [37]. Figure 9 compares attenuation curves using this expression and projections from Equation 12/15 for the pipe, electrolyte, and cp parameters listed in Table 6, where the cp system is of the impressed current type as is likely to be the case for the various parameters that are addressed ($a \cdot g$ and offset distance). Table 6 indicates that three values for f_{corr} were addressed, consistent with the fact that this parameter can vary widely for buried situations. Also, it is assumed that the anode ground bed is equivalent resistance-wise to a single spherical anode of radius 0.749 m. In each case, Equation 12/15 projects a polarized pipe potential that is non-conservative with respect to the mid-anode spacing potential determined using the inclusive equation, although the maximum difference is only 17 mV. Also, in each case the cp provided a pipe polarization in excess of 250 mV. While additional analyses are needed to determine the difference in mid-anode spacing pipe potential for a spectrum of conditions, indications to-date are that Equation 12/15 provides an acceptable approximation.

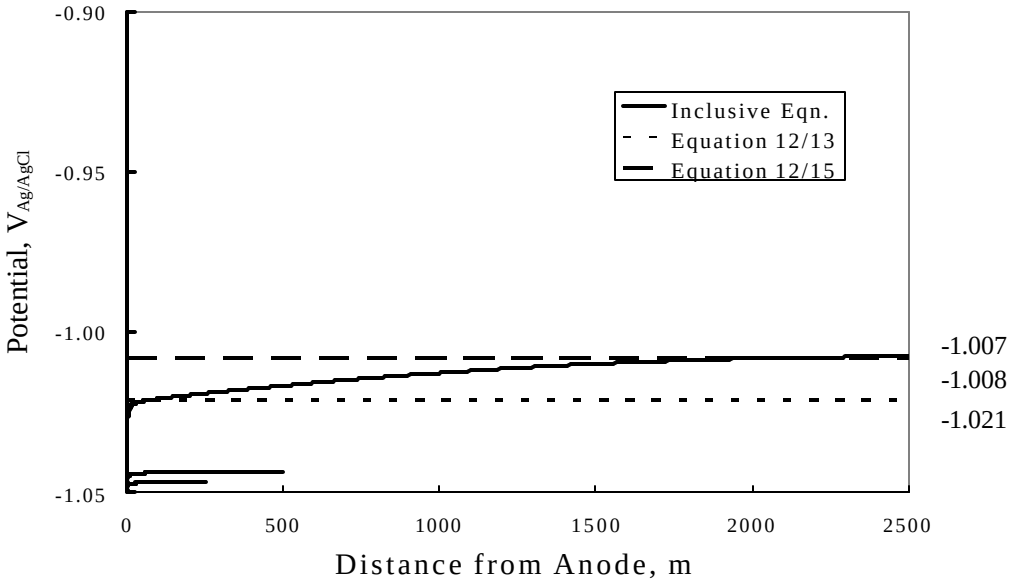

(a)

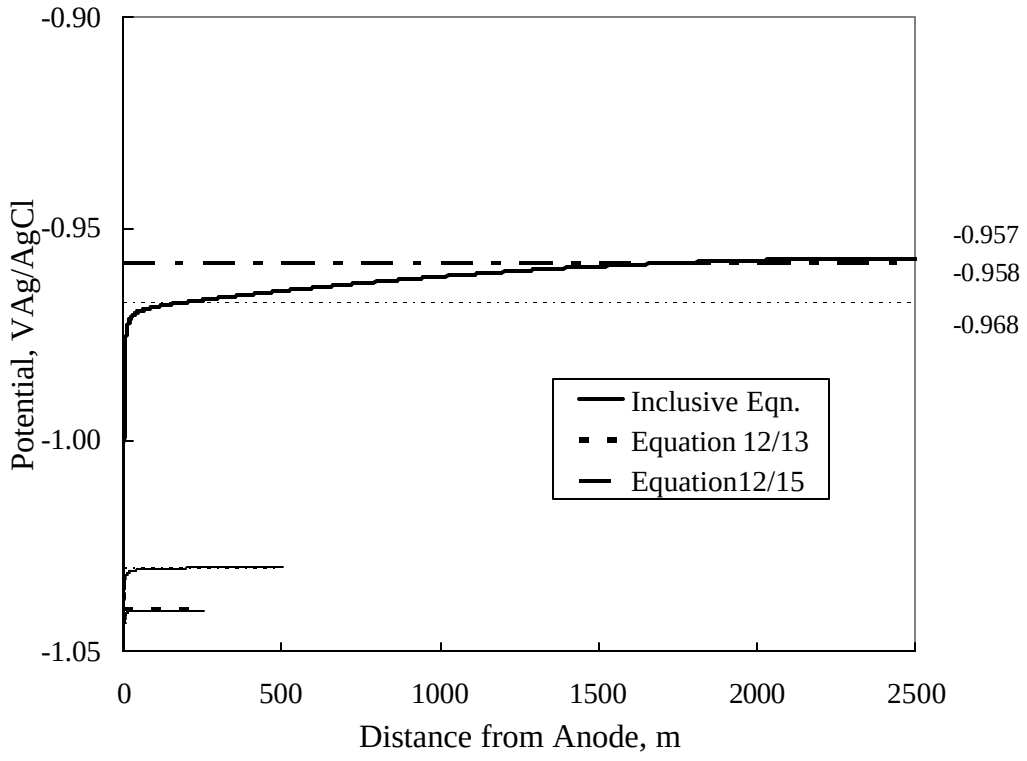

(b)

Figure 8: Comparison of potential attenuation projections using the Slope Parameter and Inclusive Equation: (a) r = 0.30 Ω·m and (b) r = 1.00 Ω·m.

Table 5: Pipe, environment, and cp parameters for a bracelet anode example.

Pipe Outer Radius, m	0.136
Pipe Inner Radius, m	0.128
Anode Radius, m	0.374
Anode Length, m	2.677
Equivalent Spherical Anode Radius, m	0.749
Polarization Resistance, a, $\Omega \cdot m^2$	17.5
Gamma, g	100
Corresponding, $\alpha\gamma$, $\Omega \cdot m^2$	1,750
Pipe Corrosion Potential, $V_{Ag/AgCl}$	-0.65
Electrolyte Resistivity, $\Omega \cdot m$	0.3, 1.0
Metallic Resistivity, $\Omega \cdot m$	1.70E-07

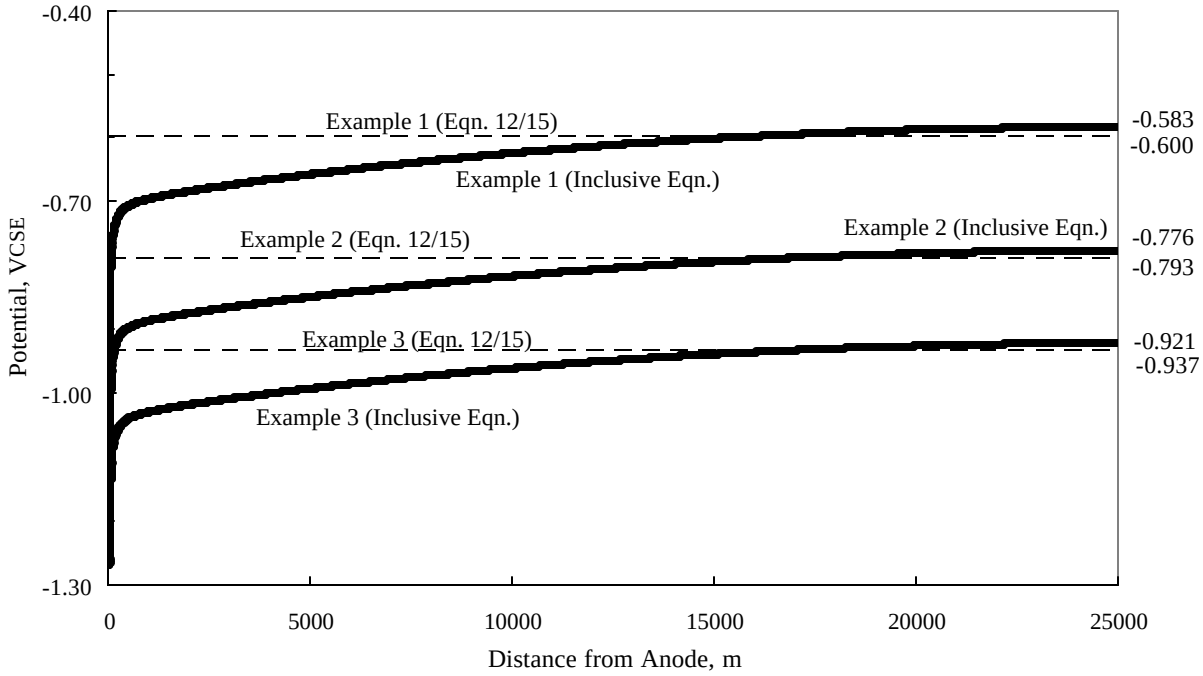

Figure 9: Comparison of potential attenuation projections using the Slope Parameter and Offset Inclusive Equation.

Summary

The Slope Parameter, which is defined as the product of total circuit resistance and cathode surface area, provides the basis for an improved approach to design and analysis of cathodic protection systems. The method is particularly useful for structures with distributed anodes in low resistivity electrolytes, and it is here that most emphasis to-date has focused. For high resistivity electrolytes or situations where anode potential and electrolyte resistivity vary with time, the method is necessarily limited to specific time analyses, since a requisite for applicability is that these factors (resisitiviy and anode potential) remain constant. Preliminary evaluations indicate that the Slope Parameter has particular utility for design of cathodic protection systems for pipelines,

where the spatially variable potential field results in complexities that do not normally occur with space-frame structures.

Table 6: Pipe, environment, and cp parameters for an offset anode bed anode example.

Pipe/CP Parameter	Example 1	Example 2	Example 3
Outer Pipe Diameter, m	0.136		
Inner Pipe Diameter, m	0.128		
Soil Resistivity, Ω·m	100		
Pipe Resistivity, Ω? m	1.70E-07		
Pipe Corrosion Potential, V_{CSE}	-0.30	-0.50	-0.65
AlphaGamma, $\Omega \cdot m^2$	17,500		
Equivalent Anode Potential, V_{CSE}	-8.50		
Equivalent Anode Spherical Radius, m	0.749		
Rectifier Voltage, V	10		
IC Anode Potential, V_{CSE}	1.50		
Anode Offset Distance, m	25		
Anode Spacing, m	50,000		

Acknowledgements

The authors are indebted to member organizations of a joint industry project, including ChevronTexaco, ExxonMobil, Shell Pipeline Company, and the Minerals Management Service for financial sponsorship of this research.

References

1. Davy, H., *Phil. Trans. Royal Soc. London*, Vol. 114, 1824, p. 151.

2. Davy, H., ibid, Vol. 114, 1824, p. 242.

3. Davy, H., ibid, Vol. 115, 1825, p. 328.

4. "Cathodic Protection Design," DnV Recommended Practice RP401, Det Norske Veritas Industri Norge AS, 1993.

5. "Corrosion Control of Steel-Fixed Offshore Platforms Associated with Petroleum Production", NACE Standard RP 0176-94, NACE International, Houston, 1994.

6. Broomfield, J.P., *Corrosion of Steel in Concrete – Understanding, Investigation, and Repair*, E&FN Spon, London, 1997, pp. 107-186.

7. Wang, W., Hartt, W. H., and Chen, S., *Corrosion*, Vol. 52, 1996, p. 419.

8. Hartt, W.H., Chen, S., and Townley, D.W., *Corrosion*, Vol. 54, 1998, p 317.

9. Townley, D. W., "Unified Design Equation for Offshore Cathodic Protection," paper no. 97473 presented at CORROSION/97, March 9-14, 1997, New Orleans.

10. "Design of Galvanic Anode Cathodic Protection Systems for Offshore Structures," NACE International Publication 7L198, NACE International, Houston, TX, 1998.

11. Fischer, K. P., Sydberger, T. and Lye, R., "Field Testing of Deep Water Cathodic Protection on the Norwegian Continental Shelf," paper no. 67 presented at CORROSION/87, March 9-13, 1987, San Francisco.

12. Kennelley, K.J. and Mateer, M.W., "Evaluation of the Performance of Bimetallic Anodes on a Deep Water Production Platform," CORROSION/93, paper no. 523, NACE, Houston, TX, 1993.

13. Wang, W, Hartt, W.H., and Chen, S., *Corrosion*, Vol. 52, 1996, p. 419.

14. Sagüés, A.A. and Powers, R.G., "Low-Cost Sprayed Zinc Galvanic Anode for Control of Corrosion of Reinforcing Steel in Marine Bridge Substructures," Final Report submitted to the Strategic Highway Research Program on Contract No. SHRP-88-ID024 by Univ. South Florida, February, 1994.

15. W. H. Hartt, *Corrosion*, Vol. 58, 2002, p. 513.

16. Standard Recommended Practice RP0290-90, "Cathodic Protection of Reinforcing Steel in Atmospherically Exposed Concrete Structures," NACE International, Houston, TX, 1990.

17. Wolfson, S.L. and Hartt, W.H., *Corrosion*, Vol. 37, 1981, p. 70.

18. Hartt, W.H., Culberson, C.H. and Smith, S.W., *Corrosion*, Vol. 40, 1994, p. 609.

19. Lin, S-H and Dexter, S.C., *Corrosion*, Vol. 44, 1988, p. 615.

20. Finnegan, J.E. and Fischer, K.P., "Calcareous Deposits: Calcium and Magnesium Ion Concentrations," paper no. 581 presented at CORROSION/89, April 17-21, 1989, New Orleans.

21. Fischer, K.P. and Finnegan, J.E., "Cathodic Protection Behavior of Steel in Sea Water and the Protective Properties of the Calcareous Deposits," paper no. 582 presented at CORROSION/89, April 17-21, 1989, New Orleans.

22. Luo, J.S., Lee, R.U., Chen, T.Y., Hartt, W.H. and Smith, S.W., *Corrosion*, Vol. 47, 1991, p. 189.

23. Mantel, K.E., Hartt, W. H. and Chen, T. Y., *Corrosion*, Vol. 48, 1992, p. 489.

24. Cox, G.C., "Anticorrosive and Antifouling Coating and Method of Application", U.S. Patent 2,200,469, 1940.

25. Foster, T., and Moores, V.G., "Cathodic Protection Current Demand of Various Alloys in Sea Water," paper no. 295 presented at CORROSION/86, March 17-2, 1986, Houston.

26. Mollan, R. and Anderson, T.R., "Design of Cathodic Protection Systems," paper no. 286 presented at CORROSION/86, March 17-2, 1986, Houston.

27. Fischer, K.P., Sydberger, T. and Lye, R., "Field Testing of Deep Water Cathodic Protection on the Norwegian Continental Shelf," paper no. 67 presented at CORROSION/87, March 9-13, 1987, San Francisco.

28. Fischer, K.P. and Finnegan, J.E., "Cathodic Protection Behavior of Steel in Sea Water and the Protective Properties of the Calcareous Deposits," paper no. 582 presented at CORROSION/89, April 17-21, 1989, New Orleans.

29. Schrieber, C.F. and Reding, J., "Application Methods for Rapid Polarization of Offshore Structures," paper no. 381 presented at CORROSION/90, April 23-27, 1990, Las Vegas.

30. Hartt, W.H., "The Slope Parameter Approach to Marine Cathodic Protection Design and Its Application to Impressed Current Systems," *Designing Cathodic Protection Systems for Marine Structures and Vehicles*, Ed. H. P. Hack, ASTM STP 1370, American Society for Testing and Materials, 1999, p. 1.

31. "Pipeline Cathodic Protection – Part 2: Cathodic Protection of Offshore Pipelines," Working Document ISO/TC 67/SC 2 NP 14489, International Standards Organization, May 1, 1999.

32. Bethune, K and Hartt, W.H., *Corrosion*, Vol. 57. 2001, p. 78.

33. McCoy, J. E., The Institute of Marine Engineers Transactions, Vol. 82, 1970, p. 210.

34. Pierson, P., Bethune, K., Hartt, W.H., and Anathakrishnan, P, Corrosion, Vol. 56, 2000, p. 350.

35. Lysogorski, D.K., Hartt, W.H., and Anathakrishnan, P, "A Modified Potential Attenuation Equation for Cathodically Polarized Marine Pipelines and Risers," paper no. 03377 to be presented at CORROSION/03, March 16-21, 2003, San Diego.

36. Lysogorski, D.K. and Hartt, W.H., "A Potential Attenuation Equation for Design and Analysis of Pipelines Cathodic Protection Systems with Displaced Anodes," paper no. 03196 to be presented at CORROSION/03, March 16-21, 2003, San Diego.

37. Hartt, W.H. and Lysogorski, D.K., "The Slope Parameter Approach in Design and Analysis of Cathodic Protection Systems," paper no. 03197 to be presented at CORROSION/03, March 16-21, 2003, San Diego.